Journal of Applied Polymer Science

Preparation and Testing of Nafion/Titanium Dioxide Nanocomposite Membrane Electrode Assembly by Ultrasonic Coating Technique

Yilser Devrim
Department of Energy System Engineering, Atilim University, 06836 Incek, Ankara, Turkey
Correspondence to: Y. Devrim (E-mail: yilser.devrim@atilim.edu.tr)

ABSTRACT: Membrane electrode assemblies with Nafion/nanosize titanium dioxide (TiO_2) composite membranes were manufactured with a novel ultrasonic-spray technique (UST) and tested in proton exchange membrane fuel cell (PEMFC). The structures of the membranes were investigated by scanning electron microscopy (SEM), X-ray diffraction (XRD), and thermogravimetric analysis. The composite membranes gained good thermal resistance with insertion of TiO_2. The SEM and XRD techniques have proved the uniform and homogeneous distribution of TiO_2 and the consequent enhancement of crystalline character of these membranes. The existence of nanometer size TiO_2 has improved the thermal resistance, water uptake, and proton conductivity of composite membranes. Gas diffusion electrodes were fabricated by UST. Catalyst loading was 0.4 (mg Pt) cm^{-2} for both anode and cathode sides. The membranes were tested in a single cell with a 5 cm^2 active area operating at the temperature range of 70°C to 110°C and in humidified under 50% relative humidity (RH) conditions. Single PEMFC tests performed at different operating temperatures indicated that Nafion/TiO_2 composite membrane is more stable and also performed better than Nafion membranes. The results show that Nafion/TiO_2 is a promising membrane material for possible use in PEMFC at higher temperature. © 2014 Wiley Periodicals, Inc. J. Appl. Polym. Sci. **2014**, *131*, 40541.

KEYWORDS: batteries and fuel cells; nanoparticles; nanowires and nanocrystals; properties and characterization

Received 30 November 2013; accepted 4 February 2014
DOI: 10.1002/app.40541

INTRODUCTION

Proton exchange membrane fuel cells (PEMFCs) are receiving attention as the most practical fuel cell candidate due to their low operating temperature, non-production of CO and suitability for electric vehicles.[1] Proton exchange membrane is the key component of the PEMFC for transferring protons from the anode to cathode as well as providing a barrier to the fuel gas crossleaks between the electrodes.[2]

Dupont's Nafion is the PEM material most frequently used for this type of application because of its high proton conductivity, excellent mechanical properties, good chemical stability, and commercial availability.[3] However, the high cost, low stability at high temperatures, and low conductivity at low humidity or high temperature limits the extent of its further application and commercialization Therefore, it is necessary to develop an alternative membrane which is less expensive and has high performance.[4,5]

Over the last decade, efforts to overcome the drawbacks of Nafion membranes have proposed various studies.[6–9] A useful approach to develop this type of membrane is to modify Nafion membranes with micron or submicron inorganic/organic additives such as SiO_2,[10] TiO_2,[11] and ZrO_2.[12] Such composite membranes have exhibited improvements in water retention and fuel cell performance at elevated temperatures. Adjemian et al.[13,14] reported on the performance and characterization of several metal oxide composites recast with Nafion. Membranes were made using SiO_2, TiO_2, Al_2O_3, and ZrO_2 improved fuel cell performance at elevated temperature and reduced humidity. The authors attributed the improvement in performance to a specific chemical interaction between the inorganic particles and the sulfonate groups in Nafion. It has been reported that inorganic fillers in polymer inorganic composite membranes are to retain water inside the membrane to improve proton conductivity.[15] The addition of an inorganic material into polymer membrane can alter and improve physical and chemical polymer properties of interest (such as elastic modulus, solvent permeation rate, tensile strength, hydrophilicity, and glass transition temperature) while retaining its important polymer properties to enable operation in the fuel cell.[16,17] The effects of composition, methods, and conditions of preparation of the composite membranes on the related performance are known; however, still additional research needs to be done in this field.

Among the inorganic materials used in this field, TiO_2 is a good candidate as hydrophilic filler for the polymer membranes because it helps to maintain a suitable hydration of the membrane under fuel cell operating conditions, and the mechanical properties are improved.[18] Watanabe et al.[19] reported the modification of Nafion PEM by incorporating nanoparticles of TiO_2 decrease the humidification requirements.

The fabrication technique of Membrane Electrode Assembly (MEA) may affect the performance and durability of PEM fuel cell. The most common gas diffusion electrode preparation techniques are sputter deposition, ion-beam assisted deposition, doctor blade, screen printing, inkjet printing, spraying, electrospraying,[20] and ultrasonic spraying. A MEA fabricated by ultrasonic spray demonstrated high performance at low Pt loading. Ultrasonic spray coating technique is replacing air spray coating technique in a wide range of industrial and R&D applications, such as photo resistor coating, solar cell industry, and fuel cell industry. Ultrasonic spray coating is a technology that is more precise, more controllable, and tighter of drop distribution. Tight drop distribution and non-clogging ultrasonic create very uniform thin films.[21]

In this article, preparation of the Nafion/TiO_2 composite membranes with TiO_2 ranging from 0 to 10 wt % were reported. The composite membranes containing nanometer sized TiO_2 were prepared by solvent casting procedure. The membranes were characterized by using X-ray diffraction (XRD), thermogravimetric analysis (TGA), water uptake, and proton conductivity measurements. Ultrasonic coating technique has been used for the fabrication of MEAs. In addition, it is the first study to use ultrasonic coating for preparing nanocomposite MEAs with different TiO_2 loading. The performance of the Nafion/TiO_2 nanocomposite membranes were compared with the Nafion in a single cell H_2–air/PEMFC at 70°C to 110°C. Compared with the commercial Nafion membrane, the obtained results have shown, on introduction of the inorganic filler, improvements in thermal stability and electrochemical performance of membranes.

EXPERIMENTAL

Materials

The commercially available 15 wt % Nafion solution (equivalent weight = 1100 g mol^{-1} SO_3H) was obtained from Ion Power. A total of 21-nm TiO_2 (anatase) was obtained from Degussa (P25) was used as received. *N-N* dimethylacetamide ($CH_3C(O)N(CH_3)_2$ DMAc) was used as received. All solvents were used high-grade reagents and without further purification.

Composite Membrane Preparation

Nafion/TiO_2 composite membranes were prepared using the recasting method. A total of 15 wt % Nafion solution was evaporated at 60°C until a dry residue was obtained. The residual Nafion resin was redissolved in a desired amount of DMAc to form a solution containing 5 wt % of Nafion. An appropriate amount of TiO_2 powder was added and to achieve good dispersion of particles sonicated for at least an hour. The resulting mixture was cast onto petri dishes and was slowly evaporated at 80°C to remove most of the solvent. The membrane was removed from the Petri dish by wetting with de-ionized water. The composites provided an opaque white membrane. The membrane thickness around 80 μm was obtained from 2.5, 5, and 10 wt % TiO_2 loading. The composite membranes containing 2.5, 5, and 10 wt % TiO_2 are classified NT-2.5, NT-5, and NT-10, respectively. TiO_2 loading was limited to 10 wt % as higher loadings produced a membrane that was subject to cracking. A recast Nafion membrane was also prepared with the same procedure for comparative study. All membranes were stored in deionized water before any test was performed.

Membrane Characterization

Thermal stability of the composite membrane was examined for the temperature range of 25°C–700°C at a heating rate of 10°C min^{-1} under nitrogen atmosphere using a Thermal Analyzer (DuPont TA 951). The XRD analysis was performed using an X-ray diffractometer (Rigaku D-MAX 2200, Japan) with CuK_α ($\lambda = 1.5406$ Å) radiation over the range $5° \leq 2\theta \leq 100°$.

Water uptake is regarded as one of the most important characteristic properties for the proton exchange membranes, which confirm the successful incorporation of hydrophilic group inside the membrane. The membranes were soaked in water at 80°C for 24 h. The excess water was wiped off gently with a foam filter, and they were then weighed immediately. Subsequently, the membrane samples were dried at 100°C in vacuum to constant weight. The water uptake was calculated using the following equation;[22]

$$\text{Water Uptake} = [(W_{wet} - W_{dry})/W_{dry}] \times 100 \ (\%) \quad (1)$$

where W_{wet} and W_{dry} are the weights of the water-swollen and dry membrane sample, respectively.

The surface morphology of nanocomposite membranes were examined in QUANTA 400F Field Emission Scanning Electron Microscope (SEM) system equipped with an energy dispersive X-ray (EDX) spectrometer. Before measurements, the samples were coated with a layer of gold to enhance electrical conduction.

Proton Conductivity Analysis. The proton conductivity of the membranes was measured by AC electrochemical impedance spectroscopy (EIS) technique over a frequency range of 1–300 kHz with an oscillating voltage using the potentiostat system (GAMRY PCL40). All measurements were performed in longitudinal direction; in air/water vapor atmosphere at 100% relative humidity (RH) with four probe EIS as a function of temperature. The specimens were prepared as 1 cm × 5 cm membrane strips and sandwiched into Pt electrode lined Teflon conductivity cell. The specimen and the electrodes were fixed by nuts and bolts. The specific conductivity [σ, (Ω cm^{-1})] was calculated on the basis of the measured resistance according to the following equation;[23]

$$\sigma = (1/R) \times (l/A) \quad (2)$$

where l is the distance between the two electrodes (cm), R is the membrane resistance (Ω), and A is the cross-sectional area of the membrane (cm^2). Proton conductivity experiments were repeated three to four times to confirm reproducibility in results.

Accelerated Chemical Degradation. The composite membrane degradation was studied by immersion in Fenton reagent (4 ppm Fe^{2+}, 3% H_2O_2) at 80°C. The initial sample weight was

measured, and the samples were put into a solution of iron (II) sulfate heptahydrate in MilliQ water (45 mL) and heated to 80°C, after which 5 mL of 30% H_2O_2 was added to the solution. The membrane samples were taken out regularly during the experiment for weighing. Washing the sample in distilled water quenched the degradation reaction, and the exposed membranes were dried before the final weight was determined.

The dimensional change was investigated by immersing the membrane into water at room temperature and 80°C for 24 h, and the changes in thickness and length were calculated from the equation,

$$\Delta t = \frac{(t - t_o)}{t_o} \quad (3)$$

$$\Delta l = \frac{(l - l_o)}{l_o} \quad (4)$$

where t_o and l_o are the thickness and length of the dried membrane, respectively; and t and l refer to these same parameters after the membrane is immersed in water for 24 h.

The titration method was used to determine the Ion Exchange Capacity (IEC) of the membranes. The membranes in the acid form (H^+) were converted to the sodium salt form by immersing the membranes in a 1.0 *M* NaCl solution for 24 h to exchange the H^+ ions with Na^+ ions. Then, the exchanged H^+ ions within the solutions were titrated with a 0.01 *N* NaOH solution.[24,25] The procedure was performed three times and the results averaged.

MEA Preparation

MEAs were fabricated by Ultrasonic Coating Technique, which was used by Devrim. The catalyst ink was prepared using the method reported in a previous article. The catalyst ink was composed of 70 wt % catalyst (the catalyst is 70 Pt wt % on Vulcan) and 30 wt % Nafion (on dry basis) in a solution of 1 : 7 ratio of water/2-propanol.[26]

The catalyst ink was ultrasonic-sprayed onto the GDLs by the Sono-Tek "Exacta-coat" ultrasonic spray instrument. The Sono-Tek "Exacta-coat" ultrasonic spray incorporate an ultrasonic atomizing nozzle, vibrating at high frequency ultrasound (120 kHz) created by piezoelectric transducers inside the nozzles' titanium housing. Liquid traveling down the center of the nozzle forms capillary waves as a result of this vibrational energy. The ultrasonic nozzles' large orifice and ultrasonic vibration make it possible to atomize high solids materials without clogging. Therefore, the dispersion of particles in solution is highly uniform throughout the entire coating process, providing the most homogenous coatings possible.[27] Coating process is fully computer controlled and can be programmed according to the coating area. The catalyst ink (15 mL) was inserted in a syringe pump before atomization in the nozzle (Accumist) and sprayed at a flow rate up to 0.5 mL min^{-1}. Various passes were performed in views of obtaining the appropriate loading. After spraying the catalyst ink onto the GDLs, MEA was prepared by pressing GDLs onto the treated membrane at 130°C and 688 N cm^{-2} for 3 min.

PEMFC Performance Tests

Performances of fabricated MEAs were measured via the PEMFC test station (TECHYS HYGO FCTS-H2ME 500). A single cell PEMFC (Electrochem) with a 5 cm^2 active area was used in the experiments. The test cell was tightened with a torque of 1.7 Nm applied to each bolt. The external load was applied by means of an electronic load (B&K Precision), which can be controlled either manually or by the computer. The current and voltage of the cell were monitored and logged throughout the operation of the cell by the fuel cell test software (TECHYS-HYGO). The fabricated MEA was placed in the test cell, and the bolts were tightened with a torque of 1.7 Nm on each bolt. The cell temperature was adjusted and the temperatures of the humidifiers and gas transfer lines were set 10°C above the cell temperature. After the preset temperatures were reached, hydrogen and oxygen are supplied to the cell at a rate of 0.1 slpm. The cell was operated at 0.5 V until it came to steady state. After steady state was achieved, starting with the open circuit voltage (OCV) value, the current-voltage data was logged by changing the load.[27]

RESULTS AND DISCUSSION

Structural Analysis

The XRD patterns of Nafion, Nafion/TiO_2 composite membranes, and TiO_2 were illustrated in Figure 1. The pattern of TiO_2 crystal powders has three crystalline characteristic peaks at 2θ of 25.34°, 37.72°, and 48.02°, as reported in the literature.[28,29] The Nafion membrane shows two main peaks at 17.5° (2θ) and 38.3° (2θ), which were consistent with those reported in literature.[30] The broad peak at 17.5° (2θ) was related to the crystalline scattering of the polyfluorocarbon chains in Nafion membranes, which overlapped the X-ray scattering from the amorphous region of the membrane at lower Bragg angles.[31] The pattern of Nafion/TiO_2 composite membranes have three crystalline characteristic peaks at 2θ of 25.42°, 37.66°, and 48.06° that is analogous with the characteristic peaks of TiO_2 crystal powders in addition to the dispersion peak of Nafion. This shift of characteristic peaks of TiO_2 in the Nafion/TiO_2 composite membrane indicates that there may be interactions between polymer and TiO_2. The specific molecular interaction between the inorganic particles and the polymer matrix was found with mass spectroscopic detection (TG-MS).[32] The interaction of Nafion in solution with the various inorganic oxides plays a vital first step in making a successful composite membrane. In the recasting process, the Nafion rods are expected to orient themselves around the metal oxide particles because of the electrostatic and chemical interactions and, after evaporation of the solvent, form a homogeneous composite membrane.

Thermal analysis

TGA results of Nafion and Nafion/TiO_2 composite membranes were reported in Figure 2. It was observed that all the membranes retain more than 90% of its weight up to a temperature of about 300°C. The results of the thermal degradation studies of Nafion membranes agree well with the results reported in the literature.[33] TGA analysis of the Nafion membrane showed three regions of weight loss. The first weight loss, between 50°C and 200°C, corresponds to the removal of moisture from the material. The TGA curve revealed a second weight-loss region between 200°C and 400°C; this corresponds to the decomposition of the $-SO_3H$ groups. The weight loss observed in the

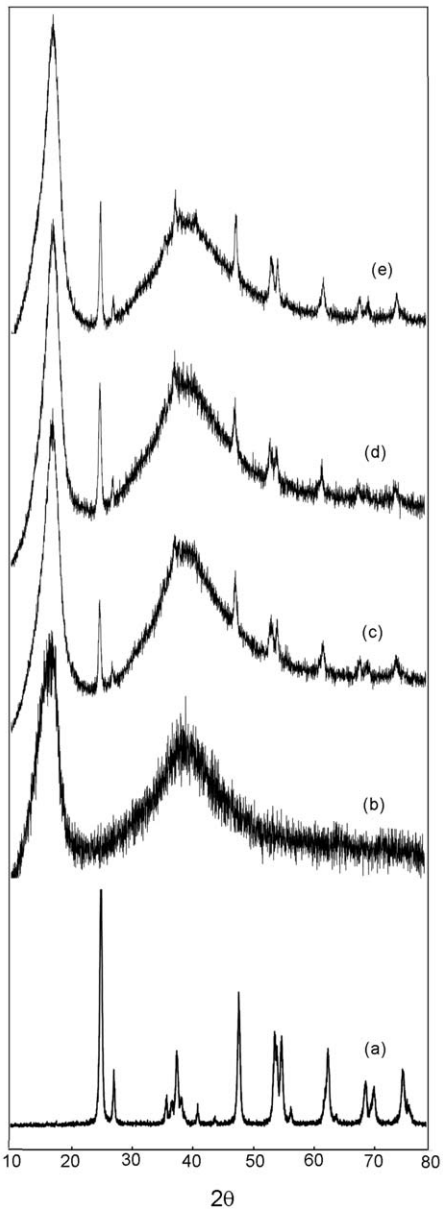

Figure 1. XRD patterns of (a) TiO_2 nanoparticle, (b) Nafion, (c) NT-2.5, (d) NT-5, and (e) NT-10 composite membranes.

perfluorocarbon region (from 400°C to 550°C) was due to the decomposition of Nafion. The thermal decomposition behavior of Nafion/TiO_2 composite membrane was similar to that of Nafion, but the major decomposition temperature of the polymer main chain shifted to a much higher temperature region. This could be attributed to the strong interaction between hydrophobic Nafion backbones and TiO_2 particles. Similar observations were made for other Nafion/TiO_2 composite membrane studies.[15,34,35] TGA results also suggest that the Nafion/TiO_2 composites have slightly higher thermal stability than Nafion.

T_g values of Nafion/TiO_2 composite membranes were obtained by Differential Scanning Calorimetry (DSC) analysis. As seen from Table I, the addition of the TiO_2 nanoparticles increased the glass transition temperature from $T_g \sim 105$°C, for the Nafion to $T_g \sim 134$°C for the composites. Incorporation of TiO_2 particles in Nafion polymer matrix would fill these free volumes and would cause need to more energy for starting segmental motions, which would make T_g to increase. Also Deng et al. reported that the TiO_2 particles act to crosslink the Nafion polymer chains. One consequence of this type of chemical interaction would be an increase in the glass-transition of the composite membrane.[36] These increases of T_g values suggest improved thermal stability and hence provide potential advantages during the PEM fuel cell operation at high temperatures.

Water uptake, IEC, and Proton Conductivity

Water uptake plays an essential role in the PEMFC performance.[37] To investigate the effect of fillers on the water retention ability of the composite membrane, the water uptakes were measured for composite membranes. Water uptake data for Nafion and Nafion/TiO_2 nanocomposite membranes in the temperature range 30°C–90°C are presented in Figure 3. The hydrophilic TiO_2 nanoparticles existed in hydrophilic domains of composite membranes decrease the water uptake of membrane. Water uptake decreases with the increase of the doping level of TiO_2 particles up to 10 wt %. This may be attributed to the distribution of TiO_2 and the availability of active sites (OH attached with TiO_2) on the surface of the composite membrane for hydrogen bonding with water. Because of the masking of hydrophilic SO_3H groups in the Nafion clusters, further increase in doping amount leads to the decrease in water uptake.[35] Water uptakes of the nanocomposite membranes were increased with temperature. This variation in water uptake was attributed to the swelling of membrane and easy penetration of water molecule in the swelled bulk matrix.[38]

Proton conductivity is an important parameter for PEMFC to assess the contribution of functional groups and structural features of polymer matrix such as water content and interaction between ionic groups towards proton conduction. The proton conductivity measurements were performed in longitudinal direction; in air/water vapor atmosphere at 100% RH with four probe EIS as a function of temperature. The proton

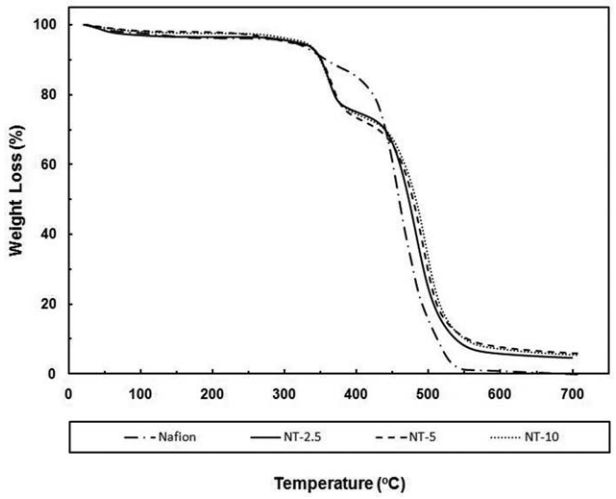

Figure 2. TGA curves of Nafion and Nafion/TiO_2 composite membranes with different TiO_2 loading.

Table I. Thermal Properties and Proton Conductivities of Nafion and Nafion/TiO_2 Composite Membranes

		Thermal properties			Proton conductivity (S cm^{-1})			
Membrane	TiO_2 loading (wt)	$T_{d,1}$ (°C)	$T_{d,2}$ (°C)	T_g (°C)	25°C	50°C	70°C	90°C
Nafion	0	355	465	105	0.130	0.185	0.208	0.227
NT-2.5	2.5	352	487	122	0.115	0.198	0.251	0.282
NT-5.0	5.0	354	494	127	0.109	0.194	0.248	0.279
NT-10	10.0	353	491	134	0.099	0.188	0.233	0.264

conductivity of the Nafion/TiO_2 nanocomposite membranes are shown in the Table I. As temperature plays a vital role in the kinetics of proton motion in the polymeric membrane and the mobility of polymer chains, all the membranes exhibited an increase in conductivity with temperature. At high temperature, the dissociation of hydrogen is promoted causing an increase of proton conductivity. However, at temperatures above 80°C, which are close to the boiling point of water, the adsorbed water inside the membrane vaporized rapidly.[30]

It is clear from the data that the proton conductivity of the composite membranes has been decreased with increasing of the TiO_2 content in composite membranes at room temperature. On the other hand, the proton conductivity of the composite membranes is higher than Nafion membrane with increasing temperature. The maximum proton conductivity at 70°C is ordered amongst the samples as follows: NT-2.5 > NT-5 > NT-10> Nafion. The highest proton conductivity of the NT-2.5 nanocomposite membrane was 0.282 S cm^{-1}, 24% higher than that of the unmodified Nafion membrane at 90°C. The improved proton conductivity could be explained by the hydrophilic nature of well-dispersed TiO_2 nanoparticles. From the conductivity data, the performance of water retention by TiO_2 nanoparticles is more effective at higher temperatures.[38] The decrease of the proton conductivity with the increase in TiO_2 content may be attributed to barrier properties of TiO_2 particles due to the non-homogenous dispersed inorganic fillers disrupt the continuum of sulfonic group clusters that are responsible for the proton motion in the Nafion membrane.[39]

It can be seen from Table II that the IEC of composite membrane have slight changes compared with that of the Nafion membrane. The IECs of NT-2.5, NT-5, and NT-10 were 0.905, 0.89, and 0.87 meq g^{-1}, whereas the IEC of the Nafion 211® was 0.915 meq g^{-1}, respectively. The IEC did not change significantly with increase in TiO_2 loading. The IEC of nanocomposite membranes is slightly lower than the Nafion. Similar to water uptake, the addition of TiO_2 into the Nafion slightly decreases the IEC of the composite membrane due to covering the Nafion active sites (sulfonic groups) and decreasing the effective number of replaceable ion exchange sites by the salts.[40,41] The greater IEC of the NT-2.5 membrane than the NT-10 membrane may be associated with the free sulfonic group of Nafion matrix in the NT-2.5 than the NT-10.

Dimensional Stability

Table II summarizes the accelerated test results of the Nafion/TiO_2 composite membranes with TiO_2 concentration of 0, 2.5, 5, and 10 wt %. Membrane durability is an important factor to achieve a long working lifetime of fuel cell. The oxidative stability of membranes was investigated using Fenton's reagent to evaluate the stability of membranes against the attack of radical species. The accelerated tests were evaluated in hot Fenton reagent for 12 and 24 h as an accelerated chemical degradation test of the membranes. The weight loss of the membranes after the testing is presented in Table II. All membranes have strong stability in oxidative media due to the structure of the polytetrafluoroethylene backbone. It can be found that all the composite membranes show slightly better performance than that of Nafion membrane after the Fenton tests. The results show that the Nafion/TiO_2 composite membrane has slightly higher stability against oxidative agents. The reason may be the role of TiO_2 in the interaction of sulfonic acid against the diffusion of H_2O_2.

The through-plane (Δt) and in-plane (Δl) dimensional changes of nanocomposite membranes were evaluated by comparing their hydrated state with the dry state. The dimensional stability of the Nafion composite membranes were increased when the inorganic content was increased. The presence of TiO_2 as inorganic fillers in the ionic clusters of Nafion matrix provides good dimensional stability. The interactions between the TiO_2 nanofiller and the Nafion host polymer are expected to give rise to dynamic crosslink, as witnessed by the improved dimensional stability of Nafion/TiO_2 membranes in comparison with the pristine Nafion. It is assumed that dynamic crosslinks are formed between the $-SO_3H$ groups of Nafion and the particles of the TiO_2 nanofiller and arise mainly from dipolar interactions.[42] A small change in the through and in-plane dimensions is desirable behavior for maintaining dimensional stability during the operation of a PEMFC.

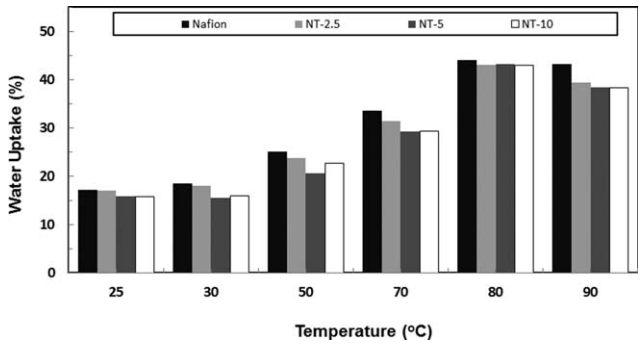

Figure 3. Effect of TiO_2 loading and temperature on water uptake of Nafion/TiO_2 composite membranes.

Table II. IEC and Accelerated Test Results of Composite Membranes

		Fenton test[a]		Dimensional stability[b] (%)			
		Retained weight (%)	Retained weight (%)	Δt	Δt	Δl	Δl
Membrane	IEC (meq g^{-1})	12 h	24 h	25°C	80°C	25°C	80°C
Nafion 212	0.915	97.2	94.5	15.51	15.8	11.93	13.76
NT-2.5	0.905	97.8	95.2	13.32	13.91	10.84	12.71
NT-5.0	0.89	98.5	96.3	12.94	13.52	10.15	11.78
NT-10	0.87	98.8	96.7	12.63	12.85	10.05	11.62

[a] Weights retained after treating the membrane in Fenton's reagent at 80°C.
[b] The dimensional change was observed by immersing the membrane into water at 25°C and 80°C.

SEM Analysis

The morphology of the Nafion/TiO_2 composite membranes was investigated by SEM analysis. Figure 4 shows the SEM images of the Nafion/TiO_2 nanocomposite membranes prepared with different TiO_2 doping levels. The composite membranes did not contain any voids or pores thus they were adequate to be used in PEM fuel cells Figure 4(a) indicates that the TiO_2 nanoparticles in the Nafion polymeric matrix have homogeneously dispersed in nanocomposite membrane with 2.5 wt % of TiO_2 loading. Significant agglomerations of titanium particles were

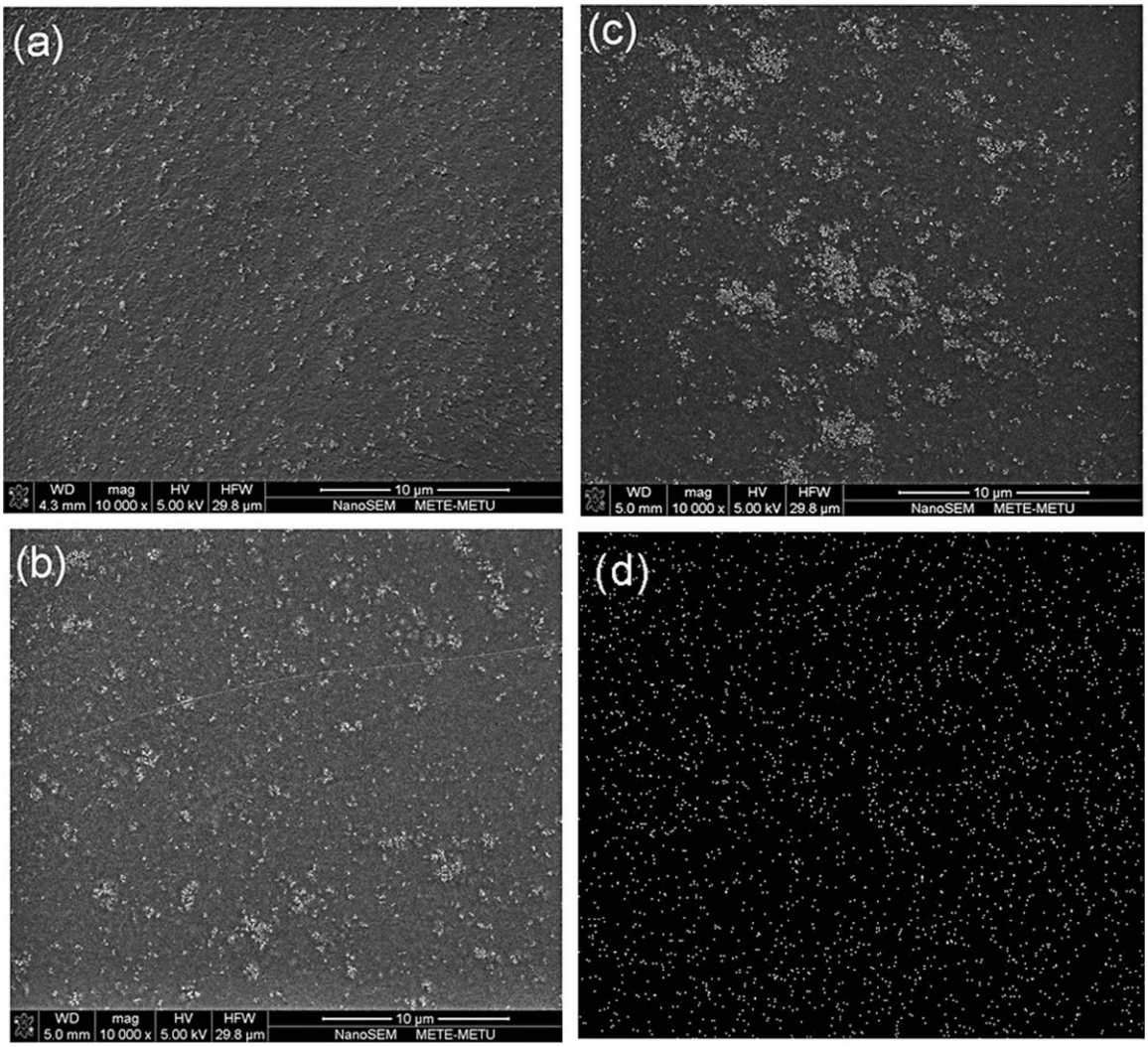

Figure 4. SEM image of (a) NT-2.5, (b) NT-5, (c) NT-10 composite membranes, and (d) EDXA mapping images of NT-2.5 composite membrane.

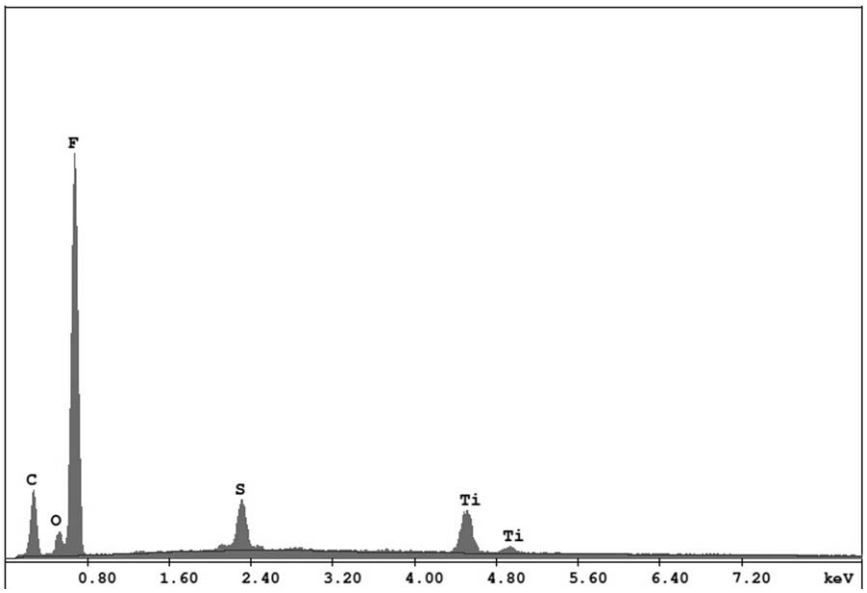

Figure 5. EDXA spectra of NT-2.5 composite membrane.

clearly visible in the Nafion/TiO_2 (10 wt %) composite membrane [Figure 4(c)]. These images show that the aggregation of TiO_2 particles is occurred at higher inorganic doping levels. The low amount of TiO_2 particles decreases the particle aggregation and formation of large particles. This observation is in compliance with the result of Amjadi et al.[7] Dispersion of the TiO_2 particles in the NT-2.5 composite membrane was studied by the EDXA mapping image. In Figure 4(d), bright dots manifest the high concentration of the TiO_2 particles. According to Figure 5, existence of the TiO_2 peak in the EDXA spectra proved the TiO_2 particles in the membrane.

SEM images of cross sections of the nanocomposite MEAs were examined before and after testing in PEM fuel cell are shown in Figure 6. Figure 6(a) shows the cross-sectional view of the MEA before fuel cell testing. The catalyst layer can be seen as narrow bright bands on both sides of the membrane. The cross section of both catalyst layers indicates that Pt catalyst was uniformly distributed. The interfaces between the nanocomposite membrane and the electrodes can be observed in the image. No gaps between the membrane and electrodes are observed. Deformation on the catalyst layer and the membrane cross section are seen clearly in Figure 6(b). Catalyst layer deformations may occur due to carbon corrosion which is prone to oxidation in the presence of Pt.[43] On the other hand it is known that the attack of HO• and HO_2• radicals produced by the incomplete reduction of oxygen on the cathode side is the main factor for the oxidative degradation of the membrane.[44]

Fuel Cell Performances

The polarization curves obtained at different TiO_2 loading for the MEAs prepared with Nafion/TiO_2 composite membrane

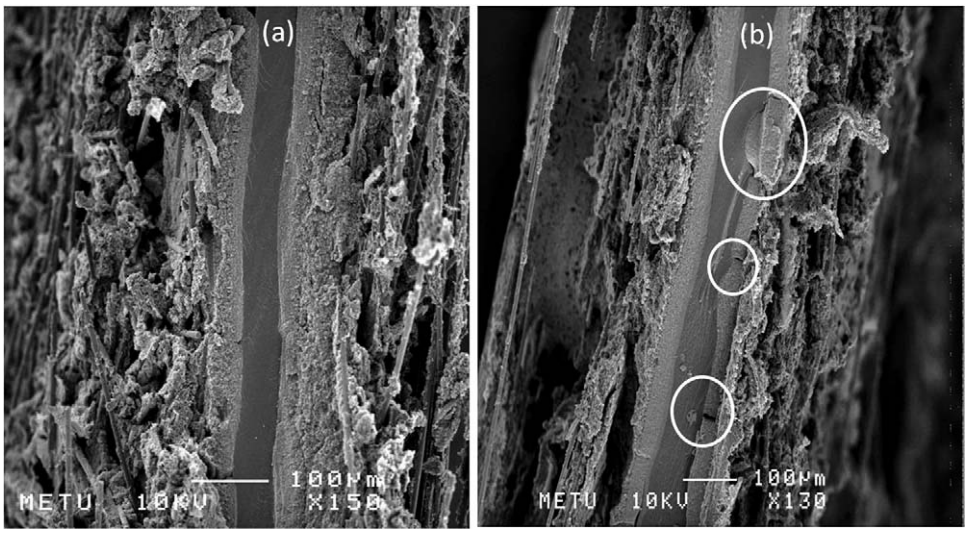

Figure 6. SEM images of the cross sections of the (a) unused MEA (b) deformation occurred on the catalyst layer after testing MEA in PEMFC.

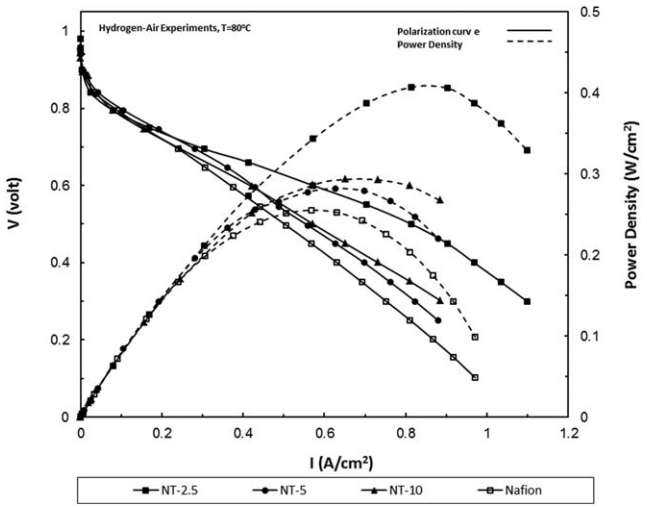

Figure 7. Effect of TiO_2 content on the PEMFC performance of composite membranes at 80°C.

are shown in Figure 7. In this study, MEAs have the same electrode structure, and the observed features can only be attributed to modifications of the membrane by the addition of TiO_2 particles. The performance efficiencies of the NT-2.5 are higher than those with 10 and 5 wt % loading of the corresponding TiO_2 fillers at 80°C. This effect is mainly due to a significantly better water retention than the bare perfluorosulfonic membrane. The current density delivered at a cell voltage of 0.6 V and the corresponding power density at 80°C for Nafion, NT-2.5, NT-5, NT-10 composite membranes and Nafion are 0.4, 0.572, 0.43, and 0.42 A cm^{-2}, and 0.16, 0.343, 0.26, and 0.25 W cm^{-2}, respectively. The further increase of the electrochemical performance may thus be achieved by appropriate tailoring of the surface characteristics of the inorganic filler. This result suggested that the higher loading of the TiO_2 particles did not lead to a higher effect on PEMFC performance as expected and is ascribed to the possible aggregation of the TiO_2 filler in the composite membranes.[11,45]

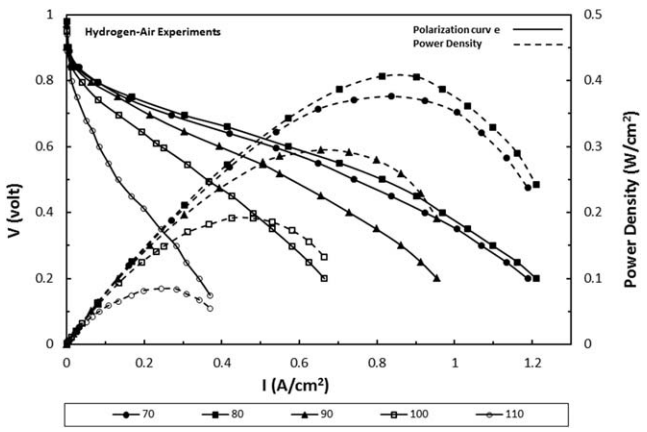

Figure 8. Effect of temperature on the PEMFC performance of NT-2.5 composite membrane.

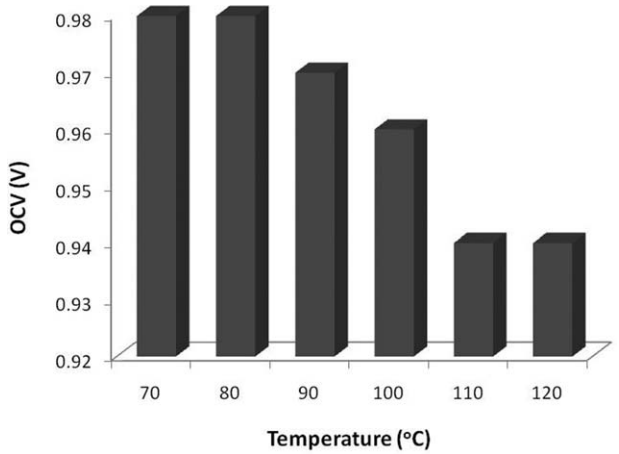

Figure 9. Effect of temperature on the OCV values of the NT-2.5 composite membrane.

The polarization curves obtained at different cell temperatures for the MEAs prepared with NT-2.5 composite membranes are shown in Figure 8. Due to water flooding and drainage issues, it was difficult to analyze the fuel cell performance under high current loads. The effect of temperature on the OCV of the NT-2.5 composite membrane can be seen in Figure 9. The decrease in OCV values could be explained by change in entropy. Because the change in entropy is negative, the open-circuit voltage output decreases with increasing temperature; the fuel cell is theoretically more efficient at low temperatures. However, other effects like mass transport and ionic conduction are faster at higher temperatures and this more than offsets the drop in open-circuit voltage.[46]

The polarization curves obtained at different TiO_2 loading for the MEAs prepared with Nafion/TiO_2 composite membranes and Nafion at 50% RH are shown in Figure 10. It can be concluded from the results that nanoparticles in both 100% and

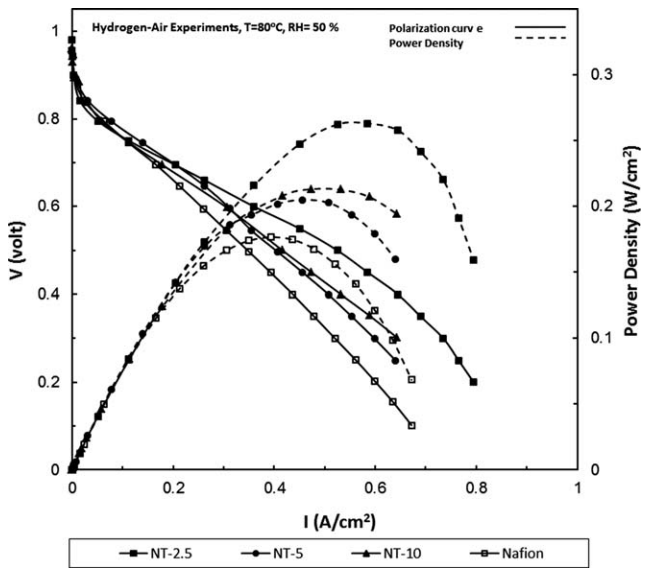

Figure 10. Effect of TiO_2 content on the PEMFC performance of composite membranes at 80°C under 50% RH.

50% RH had better performances in comparison with Nafion. This may be attributed to the hydrophilic property and enhance proton conductivity of TiO_2 nanoparticles.

CONCLUSIONS

In this work, MEAs with Nafion/TiO_2 composite membranes were successfully prepared and characterized for H2-Air PEM fuel cell application. Nafion/TiO_2 nanocomposite membranes were characterized using XRD, TGA, SEM, water uptake, proton conductivity, Fenton test, dimensional stability test, and PEMFC single cell performance. The introduction of TiO_2 particles into the membranes increased the proton conductivity; moreover, it caused the higher proton conductivity at higher temperatures. The dimensional test results show that the Nafion/TiO_2 composite membrane has slightly higher stability against oxidative agents. The morphology of the composite membranes was investigated by SEM analysis. SEM images of the Nafion/TiO_2 nanocomposite membranes indicate that the TiO_2 nanoparticles in the Nafion polymeric matrix have homogeneously dispersed in membrane with 2.5 wt % of TiO_2 loading. The aggregation of TiO_2 particles is occurred at higher inorganic doping levels. The MEA fabricated with the Nafion/TiO_2 by ultrasonic coating technique shows a significant enhancement in cell performance at high temperature. From Fenton test, it can be found that the nanocomposite membranes have better chemical stability than that of Nafion.

The membranes were tested in a single cell with a 5 cm^2 active area operating at 70°C to 110°C. Single cell PEMFC tests performed at different operating temperatures showed that Nafion/TiO_2 composite membrane is performed better than Nafion membranes. The highest performance of 0.572 A cm^{-2} was obtained for NT-2.5 membrane at 0.6 V for a H_2–air/PEMFC working at 80°C. As a result, Nafion/TiO_2 composite membranes are good alternative materials for PEMFC.

ACKNOWLEDGMENTS

This study is supported by The Scientific and Technological Research Council of Turkey (TUBITAK 1507) with Project 7110815.

REFERENCES

1. Kordesch, K.; Simader, G. Fuel Cells and Their Applications; VCH: Weinheim, **1996**.
2. Savadogo, O. *J. Power Sources* **2004**, *127*, 135.
3. Doyle, M.; Rajendran, G. In Handbook of Fuel Cell Fundamentals, Technology, and Applications; Vielstich, W.; Lamm, A., Gasteiger, H., Eds.; Wiley: England, Chichester, **2003**; p 351.
4. Alberti, G.; Casciola, M.; Massinelli, L.; Bauer, B. *J. Membrane Sci.* **2001**, *185*, 73.
5. Tricoli, V.; Nannetti, F. *Electrochim. Acta* **2003**, *48*, 2625.
6. Watanabe, M.; Uchida, H.; Seki, Y.; Emori, M.; Stonehart, P. *J. Electrochem. Soc.* **1996**, *143*, 3847.
7. Amjadi, M.; Rowshanzamir, S.; Peighambardoust, S. J.; Hosseini, M. G.; Eikani, M. H. *Int. J. Hydrogen Energy* **2010**, *35*, 1.
8. Kerres, J. A. *J. Membrane Sci.* **2001**, *185*, 3.
9. Shao, X.; Yin, G.; Wang, Z.; Gao, Y. *J. Power Sources* **2007**, *167*, 235.
10. Di Noto, V.; Gliubizzi, R.; Negro, E.; Pace, G. *J. Phys. Chem. B* **2006**, *110*, 24972.
11. Chen, S. Y.; Han, C. C.; Tsai, C. H.; Huang, J.; Chen, Y. W. *J. Power Sources* **2007**, *171*, 363.
12. Jalani, N. H.; Dunn, K.; Datta, R. *Electrochim. Acta* **2005**, *51*, 553.
13. Adjemian, K. T.; Srinivasan, S.; Bengizer, J.; Bocarsly, A. B. *J. Power Sources* **2002**, *109*, 356.
14. Adjemian, K. T.; Lee, S. L.; Srinivasan, S.; Bengizer, J.; Bocarsly, A. B. *J. Electrochem. Soc.* **2002**, *149*, A256.
15. Liu, Y.; Nguyen, T.; Kristian, N.; Yu, Y.; Wang, X. *J. Membrane Sci.* **2009**, *330*, 357.
16. Peng, F.; Lu, L.; Sun, H.; Wang, Y.; Wu, H.; Jiang, Z. *J. Membrane Sci.* **2006**, *275*, 97.
17. Peng, F.; Lu, L.; Sun, H.; Wang, Y.; Liu, J.; Jiang, Z. *Chem. Mater.* **2005**, *17*, 6790.
18. Saccà, A.; Carbone, A.; Passalacqua, E.; D'Epifanio, A.; Licoccia, S.; Traversa, E.; Sala, E.; Traini, F.; Ornelas, R. *J. Power Sources* **2005**, *152*, 16.
19. Watanabe, M.; Uchida, H.; Igarashi, H. *Macromol. Symp.* **2000**, *156*, 223.
20. Litster, S.; McLean, G. *J. Power Sources* **2004**, *130*, 61.
21. Huang, Z. H.; Shen, H. L.; Jao, T. C.; Weng, F. B.; Su, A. *Int. J. Hydrogen Energy* **2012**, *37*, 13872.
22. Kim, B. C.; Spinks, G. M.; Too, C. O.; Wallace, G. G.; Bae, Y. H.; Ogata, N. *React. Funct. Polym.* **2000**, *44*, 245.
23. Elmer, A. M.; Jannasch, P. *Polymer* **2005**, *46*, 7896.
24. Lim, Y.; Seo, D.; Hossain, Md. A.; Lee, S.; Lim, J.; Jang, H.; Hong, T.; Kim, W. *Electrochim. Acta* **2012**, *118*, 18.
25. Lei, Z.; Sanjeev, M. *J. Electrochem. Soc.* **2006**, *153*, A1062.
26. Devrim, Y.; Erkan, S.; Baç, N.; Eroğlu, I. *Int. J. Hydrogen Energy* **2012**, *37*, 16748.
27. Millington, B.; Whipple, V.; Pollet, B. G. *J. Power Sources* **2011**, *196*, 8500.
28. Staiti, P.; Arico, A. S.; Baglio, V.; Lufrano, F.; Passalacqua, E.; Antonucci, V. *Solid State Ionics* **2001**, *145*, 101.
29. Li, Y.; Sun, X.; Li, H.; Wang, S.; Wei, Y. *Powder Technol.* **2009**, *194*, 149.
30. Cele, N.; Ray, S. S. *Macromol. Mater. Eng.* **2009**, *294*, 719.
31. Staiti, P.; Arico, A. S.; Baglio, V.; Lufrano, F.; Passalacqua, E.; Antonucci, V. *Solid State Ionics* **2001**, *145*, 101.
32. Adjemian, K. T.; Dominey, R.; Krishnan, L.; Ota, H.; Majsztrik, P.; Zhang, T.; Mann, J.; Kirby, B.; Gatto, L.; Velo-Simpson, M.; Leahy, J.; Srinivasan, S.; Benziger, J. B.; Bocarsly, A. B. *Chem. Mater.* **2006**, *18*, 2238.
33. Samms, S. R.; Wasmus, S.; Savinell, R. F. *J. Electrochem. Soc.* **1996**, *143*, 1498.

34. Shao, Z. G.; Xu, H.; Li, M.; Hsing, I. M. *Solid State Ionics* **2006**, *177*, 779.

35. Barbora, L.; Acharya, S.; Verma, A. *Macromol. Symp.* **2009**, *277*, 177.

36. Antonucci, P. L.; Arico, A. S.; Cret, P.; Ramunni, E.; Antonucci, V. *Solid State Ionics* **1999**, *125*, 431.

37. Deng, Q.; Moore, R. B.; Mauritz, K. A. *J. Appl. Polym. Sci.* **1998**, *68*, 747.

38. Tripathi, B. P.; Kumar, M.; Shahi, V. K. *J. Membrane Sci.* **2009**, *327*, 145.

39. Gierke, T. D.; Munn, G. E.; Wilson, F. C. *J. Polym. Sci.* **1981**, *19*, 1687.

40. Barbora, L.; Acharya, S.; Singh, R.; Scott, K.; Verma, A. *J. Membrane Sci.* **2009**, *326*, 721.

41. Park, C. H.; Kim, H. K.; Lee, C. H.; Park, H. B.; Lee, Y. M. *J. Power Sources* **2009**, *194*, 646.

42. Noto, V. D.; Bettiol, M.; Bassetto, F.; Boaretto, N.; Negro, E.; Lavina, S.; Bertasi, F. *Int. J. Hydrogen Energy* **2012**, *37*, 6169.

43. Rangel, C. M.; Silva, R. A.; Paiva, T. I. *J. New Mater. Electrochem. Syst.* **2009**, *12*, 119.

44. Liu, G.; Zhang, H.; Hua, J.; Zhai, Y.; Xua, D., Shao, Z. *J. Power Sources* **2006**, *162*, 547.

45. Chalkova, E.; Fedkin, M. V.; Wesolowski, D. J.; Lvov, S. N. *J. Electrochem. Soc.* **2005**, *152*, A1742.

46. Tian, G.; Wasterlain, S.; Endichi, I.; Candusso, D.; Harel, F.; François, X.; Péra, M. C.; Hissel, D.; Kaufmann, J. M. *J. Power Sources* **2008**, *182*, 449.